DOE/NASA/1040-15
NASA TM-81534

CREEP-RUPTURE BEHAVIOR OF SEVEN IRON-BASE ALLOYS AFTER LONG TERM AGING AT 760° IN LOW PRESSURE HYDROGEN

Walter R. Witzke and Joseph R. Stephens
National Aeronautics and Space Administration
Lewis Research Center

August 1980

Prepared for
U.S. DEPARTMENT OF ENERGY
Conservation and Solar Energy
Office of Transportation Programs

NOTICE

DOE/NASA/1040-15
NASA TM-81534

CREEP-RUPTURE BEHAVIOR OF SEVEN IRON-BASE ALLOYS AFTER LONG TERM AGING AT 760° C IN LOW PRESSURE HYDROGEN

Walter R. Witzke and Joseph R. Stephens
National Aeronautics and Space Administration
Lewis Research Center
Cleveland, Ohio 44135

August 1980

Work performed for
U.S. DEPARTMENT OF ENERGY
Conservation and Solar Energy
Office of Transportation Programs
Washington, D.C. 20545
Under Interagency Agreement EC-77-A-31-1040

SUMMARY

Candidate iron-base alloys for heater tube application in the Stirling automotive engine were aged at 760° C for 3500 hours in a low pressure argon or hydrogen atmosphere to determine the effect on mechanical behavior. The seven alloys evaluated were N-155, 19-9DL, 316SS, Nitronic 40, A286, Incoloy 800H, and RA330. Aging produced no appreciable changes in alloy grain size but did promote increased density and growth of precipitate particles in the grains and grain boundaries. Tensile properties were generally degraded by aging, with ductility and strength changes being influenced by grain structure. Aging also decreased creep-rupture strength, with coarse grain materials being more susceptible to strength loss. The presence of hydrogen during aging did not contribute significantly to creep strength degradation in the coarse grain alloys but did result in extensive strength losses in fine grain alloys. Based on current criteria for the Mod I Stirling engine, the N-155 and 19-9DL alloys were the only alloys in this study with strengths adequate for heater tube service at 760° C.

E-486

INTRODUCTION

A materials technology program is currently underway at NASA Lewis Research Center to provide materials support for the DOE/NASA Stirling Engine Systems Project. The materials program is directed towards meeting the requirements of the high temperature components of the Stirling engines. The most critical component is the heater head which consists of the cylinders, tubing, and regenerators. The major high temperature materials requirements and the current state-of-the-art of metals and ceramics are described in recent assessments of Stirling engine materials technology (refs. 1 and 2).

The purpose of this investigation was to evaluate potential alloys for use in the heater tube portion of the heater head. The evaluation examined changes in mechanical behavior, particularly creep-rupture, as a result of long term exposure to low pressure hydrogen (H_2) at 760° C (near the maximum temperature anticipated in early versions of the Stirling automotive engine). Aging in an argon (Ar) atmosphere was also included to provide baseline data. Creep testing of the more promising alloys has been scheduled to be conducted in high pressure hydrogen at a later date, meanwhile air creep testing of the aged candidate alloys should indicate potential alloy strength losses due to aging and hydrogen exposure.

Candidate heater tube alloys for a practical Stirling automotive engine are expected to meet requirements such as high strength at high temperatures, compatability with hydrogen, oxidation resistance, ability to operate under cyclic conditions for several thousand hours, as well as low cost. Superalloys based on cobalt, nickel, or iron would be considered applicable because of their high strength at high temperature along with good oxidation resistance. The use of cobalt, however, involves a number of drawbacks including high cost, total dependence on foreign sources, and lack of world production capability to meet the large amount of cobalt required for this potential commercial application. Nickel is also a high cost, strategic element but more readily available than cobalt. The potential of nickel-base alloys is further reduced since limited testing of creep properties in high pressure hydrogen indicated that nickel-base alloys are degraded by hydrogen whereas iron-

base alloys exhibit little or no degradation (ref. 3). Therefore, the lower cost iron-base alloys may be more suitable for this Stirling automotive engine application despite a normally lower strength capability than nickel-base alloys.

Heater tubes for current prototype Stirling automotive engines are fabricated from N-155, an iron-base alloy (ref. 4). This alloy is available as tubing and has creep and corrosion properties suitable for this application. Unfortunately, N-155 is relatively expensive because of its high content of cobalt. Consequently other iron-base alloys of lower cost with adequate strengths, oxidation resistance, and other requirements have been sought to replace N-155.

This report evaluates the mechanical behavior of seven iron-base alloys (including N-155) before and after long term (3500 hr) aging at 760° C in Ar and H_2 atmospheres. Tensile properties at 25, 425, and 760° C are given. Creep-rupture properties are presented for unaged materials at 705° to 870° C and at 760° and 815° C for aged materials. Microstructural changes due to aging are discussed.

EXPERIMENTAL PROCEDURE

Compositions of the seven iron-base alloys used in this investigations are listed in Table I. All alloy materials were supplied in the form of sheet which ranged in thickness from 0.64 to 1.63 mm. Table II lists the heat treatment for each alloy that resulted in the "unaged" condition. Two of the alloys, 19-9DL and A286, were tested in several heat treat conditions. These heat treatments provided an opportunity to evaluate fine and coarse grain structures. The fine grain structures (<15 μm) resulted from heat treatments normally recommended for optimum short-time properties (ref. 5). The coarse grain structures, are associated with improved high temperature creep resistance (refs. 5 and 6) and result from high solution treatment temperatures. Test specimens were die stamped from each sheet material, providing a reduced section 9.5 mm wide by 31.8 mm long.

Long term aging of the test specimens was conducted in cylindrical stainless steel chambers heated by external resistance element furnaces. The aging treatments were conducted at 760 ± 15° C for 3500 hours. Flowing argon or hydrogen atmospheres were maintained in the chambers at a gage gas pressure of 30-60 kPa. Commercial high purity hydrogen, having a dew point of -64° C and containing 44 ppm oxygen and 1170 ppm nitrogen, was passed through a palladium purifier prior to entering the aging chamber.

Tensile and creep-rupture tests were conducted in air. Tensile properties were determined at room temperature, 425°, and 760° C at a crosshead speed of 1.27 mm/min. Constant load creep-rupture tests were conducted at 705°, 760°, 815°, and 870° C in conventional beam-loaded machines. Strain measurements during creep were determined from the movement of an extensometer attached to the reduced section of the specimens and converted to an electrical signal by means of a linear variable differential transformer. Test temperatures were measured by Pt/Pt-13 Rh thermocouples attached to the specimen reduced section.

The longitudinal microstructure of each of the alloy sheet materials in the unaged and long term aged conditions were studied by light microscopy. Average grain sizes were determined using the line intercept method. Fracture surfaces were examined with a scanning electron microscope.

RESULTS AND DISCUSSION

Microstructure

The iron-base alloys were tested in three conditions: unaged, Ar aged, and H_2 aged. The unaged condition resulted from the heat treatment listed for each alloy in Table II. The Ar aged and H_2 aged conditions resulted from exposure of the unaged alloy structure to a temperature of 760° C for 3500 hours in an atmosphere of Ar or H_2. Hydrogen analyses of the alloys before and after H_2 aging in Table III indicated all alloys except N-155 increased in H_2 content. For example, the H_2 aging increased the H_2 content in Nitronic 40 from 1.8 ppm to 7.1 ppm. (The reduction in H_2 content for N-155 following aging was confirmed in additional short-term H_2 aging tests.) It is further shown in Table III that, after air creep testing, H_2 content decreased apparently due to diffusion of H_2 out of the specimen. The H_2 contents of A286 were consistent with those for a similar hydrogen aging embrittlement study on this alloy (ref. 7).

Microstructures of the various alloys in the unaged condition are shown in Figs. 1, 2(a), and 2(d). Typical microstructures before and after Ar and H_2 aging are illustrated for 19-9DL in Fig. 2. The carbide precipitates visible in the "unaged" HT-1 condition of 19-9DL in Fig. 2(a) were effectively dissolved in the 1204° C solution annealing treatment used for unaged HT-2 in Fig. 2(d) (ref. 8). Changes observed in those 19-9DL microstructures are primarily related to the growth and coalescence of the carbide particles, notably in the grain boundaries. Aging changes in the other alloys included (a) intermetallic as well as interstitial precipitation (e.g. Ni_3Ti in A286, carbides in 19-9DL), (b) particle growth and coalescence in the grain boundaries but to a similar or lesser degree than 19-9DL (see A286, 316SS, Nitronic 40), and (c) increased particle density and growth within the matrix (N-155, RA330, Incoloy 800). Measurements of average grain diameter are listed in Table IV and show that changes in grain size due to long term aging in Ar or H_2 were not significant.

Tensile Behavior

The tensile properties of the alloys at 25°, 425°, and 760° C in the unaged and aged conditions are presented in Table V. As shown in Fig. 3(a) strengths at room temperature changed little as a result of aging except that losses in strength as high as 50 percent were noted for fine grain (HT-1, HT-2) A286. (Fine grain is defined here as < 15 μm average grain diameter. See Table IV.) In Fig. 3(b) yield strength losses at 760° C due to aging were observed in several alloys, however, N-155, 316SS, and coarse grain A286 improved in yield strength by 30-60 percent following aging. Although the A286 with fine grains (HT-1, HT-2) exhibited strength losses when aged and the coarse grain A286 (HT-3) showed strength gains, all of the resultant aged products for this alloy material at a given temperature had roughly the same level of yield strength. No loss or gain in strength could be attributed directly to the hydrogen aging atmosphere.

Changes in tensile ductility (elongation) in response to aging varied with each alloy (Fig. 3). The room temperature ductilities of N-155, 19-9DL, A286 (HT-3), and Nitronic 40 were reduced by 50 percent or more due to aging whereas the other alloy materials experienced relatively little change in elongation.

Fracture surface examination of the Nitronic 40 alloy revealed the ductile nature of the unaged room temperature tensile specimen as indicated by dimpling in Fig. 4 (a); the H_2 aged condition in Fig. 4 (b) showed no dimpling and failed intergranularly with some transgranular cleavage. Particles approximately 1 to 3 μm in diameter were noted among the dimples of the Nitronic 40 fractures. In contrast, the A286 (HT-3) alloy fractures revealed considerable dimpling in both unaged and H_2 aged conditions, Figs. 4(c) and (d); however, the unaged surface did not indicate the intergranular separation suggested for the H_2 aged fracture surface. While the yield strength of the Nitronic 40 was reduced along with ductility as a result of H_2 aging, the yield strength of the A286 (HT-3) tended to increase as H_2 aging lowered its ductility. At 760° C, all alloys except 316SS had improved ductility after aging. Hydrogen aging resulted in slightly greater ductility in coarse grain alloys at 25° and 425° C (Table V) as compared to aging in argon while the reverse trend was observed at 760° C. Fine grain alloys generally responded in an opposite manner to coarse grain alloys regarding the effect of a hydrogen aging atmosphere on tensile ductility.

Creep-Rupture Behavior

Base line data derived from creep-rupture tests of the unaged alloys at 705°-870° C as well as results from similar tests of aged materials at 760° and 815° C are given in Table VI. The effects of stress on the minimum creep rate and on the rupture life of unaged alloys at 760° and 815° C are presented in Figs. 5 and 6. For comparison, the creep-rupture results for the Ar aged and H_2 aged specimens are included on these figures.

Using multiple linear regression analysis, activation energies for creep were determined for each alloy in the unaged condition based on minimum creep rates as well as rupture lives. These activation energy values are listed in Table VII along with stress exponents and constants for the following relationships:

$$\ln \dot{\varepsilon}_m = \ln k_1 + n_1 \ln \sigma + Q_1/RT \qquad (1)$$

$$\ln t_R = \ln k_2 + n_2 \ln \sigma + Q_2/RT \qquad (2)$$

where $\dot{\varepsilon}_m$ is the minimum creep rate (sec^{-1}), t_R is rupture life (hr), k_1 and k_2 are constants, n_1 and n_2 are stress-term exponents, σ is stress (MPa), R is gas constant (8.314 J/K-mol), T is absolute temperature (K), and Q_1 and Q_2 are activation energies (J/mol) (refs. 6 and 9). Equations (1) and (2) along with the values in Table VII are useful in predicting rupture lives and minimum creep rates within the present test conditions but the reliability of extrapolations beyond these conditions is not recommended.

Heat treatments changed the structures of 19-9DL and A286 so that as grain size increased their creep resistance also increased. The influence of other factors in these heat-resisting alloys, such as precipitate density, precipitate size, etc., however, may overshadow the effect of grain size, complicat-

ing the establishment of a relationship between creep behavior and microstructure in these alloys.

The maximum creep rates of unaged A286 alloy materials are plotted in Fig. 5 (f, g, and h) with two slopes. Each slope represents the best fit for a given stress region and the change in slope suggests a change in creep mechanism. The minimum creep rate equation for each slope is given in Table VII by the coefficients (activation energy, stress exponent, and ln k) and is valid for the stress range given. Examination of Table VII indicates that two separate slopes describe the data for the 316SS and Nitronic 40 alloys between 705° and 815° C for the rupture life equation as well as the minimum creep rate equation.

In showing the creep behavior of the aged materials in Figs. 5 and 6 it was assumed that long term aging resulted in creep properties that were displaced from but paralleled those of the unaged alloy. This would imply that structural changes due to aging would not alter the activation energy or stress exponent terms but would change the values of the constant k in equations (1) and (2). Based on the results for Nitronic 40 in Figs. 5(e) and 6(e), it appears reasonable to make a similar assumption that, where the presence of hydrogen causes changes in creep behavior in addition to those due to aging per se, the H_2 aged creep properties also will parallel those of the unaged alloy.

The effect of long term aging on creep strength is further illustrated in Fig. 7, which shows gain or loss in the 1000-hour rupture strength due to aging in argon and hydrogen for test temperatures of 760° and 815° C. Aging in argon produced increases or relatively little change in the 760° C rupture strengths of 19-9DL (HT-1), A286 (HT-1 and HT-2), and Nitronic 40, namely those alloys with grain sizes less than 15 μm. In contrast, aging in hydrogen had a definite negative effect on the strength of these fine grain materials, particularly Nitronic 40. Improvements in the 815° C rupture strengths among the 19-9DL and A286 alloys suggest a recovery process may occur in the fine grain microstructure at this higher temperature.

The rupture strengths of the alloys having grain sizes larger than 15 μm were all degraded by aging. The presence of hydrogen during aging did not contribute further to the degradation. Strength recovery at 815° C was noted primarily in the large grain A286 alloy.

It is apparent that aging per se was more damaging to coarse grain alloys than those with a fine grain structure. The low pressure hydrogen atmosphere did not significantly influence the aging results of coarse grain alloys but did cause additional degradation of strengths in some fine grain alloys, namely Nitronic 40, A286 (HT-1, HT-2) but not 19-9DL (HT-1). Nitronic 40 was particularly susceptible to rupture strength loss after aging in hydrogen. It has not been determined whether the fine grain structure of the Nitronic 40 alone was responsible or whether compositional factors also contributed to this H_2 aging loss.

Elongation measurements following rupture generally indicated increased ductility to rupture with increased stress at constant temperature, over the range of loads applied to unaged alloys in this study. Nitronic 40 and 19-9DL (HT-1) differed from the other alloys in that the ductilities were observed to

go through a minimum at intermediate stresses. For example, at 815° C the rupture elongation of Nitronic 40 was at its lowest, 84 percent, at stresses of 55-69 MPa while at 21 and 83 MPa the elongations were 117 percent and 100 percent, respectively.

As expected the fine grain alloy materials were considerably more ductile than the coarse grain. Despite their lower elongations on rupture, the coarse grain materials had longer rupture lives due to their greater resistance to creep (lower creep rates). Fine grain A286 (HT-1) when tested at 760° C with a stress of 103 MPa ruptured after 59 hours with 38 percent elongation, whereas the coarse grain A286 (HT-3) broke after 665 hours with only 7 percent elongation.

The apparent effect of the long term aging was to increase rupture ductility along with an increase in creep rate and therefore a resultant decrease in rupture life. The N-155 alloy tested at 760° C and 138 MPa increased from an unaged elongation of 13 percent to 26 percent after Ar aging and to 51 percent after H_2 aging with rupture lives of 139, 87, and 61 hours, respectively.

Engine Requirements and Alloy Selection

The design criteria for the Mod I Stirling automotive engine at startup requires a maximum yield stress in the heater tubes of 102 MPa at the operating temperature (ref. 10). At 760° C the alloys in this investigation with yield strengths greater than 102 MPa in the unaged and aged conditions are N-155, 19-9DL, Nitronic 40, A286, and RA330.

At full power operation the Mod I engine design (ref. 10) requires the hydrogen working fluid to have a mean temperature and pressure of 720° C and 15 MPa, The design criteria includes a safety factor of 1.5; thus the design stress needed for a target rupture life of 4000 hours would be about 58.5 MPa. The mean operating temperature 720° C is based on a maximum temperature of 770° C on the front side facing the combustor flame and a 670° C temperature on the back side. Therefore, heater tube alloys in the MOD I engine must have rupture lives of at least 4000 hours for a stress of 58.5 MPa at 770° C.

In Fig. 8 the temperature dependence is shown for extrapolated 4000 hour rupture strengths of the four strongest alloys in this study. Two unaged alloys, N-155 and the coarse grain 19-9DL (HT-2), clearly satisfy the Mod I engine long term strength requirements. We can assume that aging of the heater tubes will occur during engine operation; reductions in strength could be similar to those noted herein. Even with present aging effects included, N-155 and 19-9DL would retain adequate strength for the 4000 hour rupture strength requirement. The coarse grain A286 (HT-3) alloy also qualifies in the unaged condition, but with any strength loss A286 would not prove adequate for this design criteria (note that up to 40 percent loss with preaging was experienced in this study). The 4000 hour rupture strength of the Incoloy 800H alloy - as well as each of the remaining alloys - would not be sufficient for these heater tube requirements. Therefore, the design requirements for the Mod I engine heater tubes are met by N-155, 19-9DL and A286 although, as aging progresses, the A286 alloy would probably not retain adequate rupture strength.

It should be noted that the operating stress requirement to which the alloy strengths are compared reflects operating at maximum pressure for the life of the engine. This is a very conservative requirement and places an undue burden on the alloy specifications. A more realistic requirement based on a 55 percent urban- 45 percent Highway Driving Cycle is currently being considered for the Mod II Stirling engine. This approach will reduce the strength requirement by more than a factor of two, thus making several additional alloys attractive for the heater tube application.

CONCLUDING REMARKS

This study has shown that long term aging generally degrades the tensile and creep-rupture properties of candidate iron-base heater tube alloys. When properly heat treated, 19-9DL has the best potential of the group of commercially available iron-base alloys evaluated to meet the current design requirements for heater tubes in the Mod I Stirling automotive engine. The 19-9DL alloy would be a relatively inexpensive substitute for the cobalt-containing N-155 alloy presently used in prototype Stirling automotive engines. To further increase the tensile and creep properties of 19-9DL for this purpose, modifications in composition as well as heat treatment should be investigated to improve and optimize the alloy structure, as well as other properties such as corrosion and oxidation resistance.

CONCLUSIONS

Based on the mechanical behavior of seven iron-base alloys evaluated before and after aging for 3500 hours at 760° C the following was concluded:

1. N-155 and 19-9DL are the only alloys in this study with adequate rupture strength to meet the design requirements for heater tubes in the Mod I Stirling automotive engine. Based on an actual driving cycle, lower rupture strength requirements may allow the inclusion of A286 and other alloys.

2. Aging per se reduces creep-rupture strength with coarse grain alloys being more susceptible to strength losses due to aging.

3. The presence of hydrogen during aging significantly affects the creep-rupture strength of fine grain alloys but does not contribute significantly to strength degradation due to aging in coarse grain alloys.

4. Changes in tensile ductility and yield strength occur as a result of long term aging, but hydrogen and argon aging atmospheres do not produce appreciably different tensile properties.

REFERENCES

1. Stephens, J. R.; Witzke, W. R.; Watson, G. K.; Johnston, J. R.; and Croft, W. J.: Materials Technology Assessment for Stirling Engines. CONS/1011-22, NASA TM-73789, 1977.

2. Stephens, J. R.: Stirling Materials Development. Highway Vehicle Systems Contractors' Coordination Meeting, CONF-7904105, 1979, pp. 262-272.

3. Harris, J. A., Jr.; and Van Wanderham, M. C.: Properties of Materials in High Pressure Hydrogen at Cryogenic, Room, and Elevated Temperatures. (FR-5768, Pratt and Whitney Aircraft, Contract NAS8-26191.) NASA CR-124394, 1973.

4. Assessment of the State of Technology of Automotive Stirling Engines. (MTI 79ASE77RE2, Stirling Systems Division, Mechanical Technology Incorporated; Contract DEN3-32.) (DOE/NASA/0032-79/4, NASA CR-159631, 1979.

5. Heat Treating of Heat-Resisting Alloys. Metals Handbook, Taylor Lyman, ed. Vol. 2. Eighth ed. Am. Soc. Met., 1964, pp. 257-268.

6. Garofalo, Frank: Fundamentals of Creep and Creep-Rupture in Metals. MacMillan Co., 1965.

7. Gray, H. R.: Embrittlement of Nickel-, Cobalt-, and Iron-Base Superalloys by Exposure to Hydrogen. NASA TN D-7805, 1975.

8. Microstructure of Wrought Heat-Resisting Alloys. Metals Handbook. Vol. 7. Eighth ed. Am. Soc. Met., 1972, pp. 157-176.

9. Conway, J. B.: Numerical Methods for Creep and Rupture Analyses. Gordan and Breach Sci. Publ., Inc., 1967.

10. Automotive Stirling Engine Development Program NASA Contract No. DEN3-32.

TABLE I. - VENDOR ANALYSES OF IRON-BASE ALLOYS

	Element, percent by weight												
Alloy	Fe*	Cr	Ni	Co	Mn	Si	W	Mo	Cb+Ta	Al	Ti	C	Other
N-155	30	21.3	19.5	19.2	1.3	0.7	2.9	2.8	1.1			0.11	0.13N
19-9DL	65	18.3	10.5		1.1	.7	1.2	1.3	.5		0.2	.31	
316SS	65	17.5	13.3		1.3	.5		2.1				.014	
Nitronic 40	64	20.1	6.8		8.6	.2						.03	.31N
A286	53	15	26		1.4	.4		1.3		0.2	2.2	.05	.26V
Incoloy 800H	45	20.4	32.5		.8	.3				.4	.4	.06	
RA330	43	19.7	34.6	.4	1.8	1.1		.1				.025	

*Remainder.

TABLE II. - HEAT TREATMENT OF IRON-BASE ALLOYS

Alloy	Thickness, mm	Heat Treatment ("unaged" condition)
N-155	1.02	AMS-5532B (Sol'n ann. 1176°C/rapid air cool or water quench)
19-9DL	.64	HT-1 Sol'n ann. 982°C/3min/in vac/He quench age 648°C/2 hr/fast furnace cool
		HT-2 Sol'n ann. 1204°C/10 min/in vac/fast furnace cool
316SS	1.60	Sol'n ann. 1093°C/3 min/in vac/He quench
Nitronic 40	1.27	AMS-5595 (Sol'n ann. 1065°C/rapid air cooling)
A286	.64	HT-1 Sol'n ann. 982°C/3 min/in vac/He quench age 718°C/16 hr/fast furnace cool
		HT-2 Sol'n ann. 982°C/30 min/in vac/fast furnace cool age 718°C/16 hr/fast furnace cool
		HT-3 Sol'n ann. 1148°C/10 min/in vac/fast furnace cool
Incoloy 800	1.63	Sol'n ann. 1121°C/1 hr/in vac/fast furnace cool
RA330	.89	AMS-5592 (Sol'n ann. 1204°C/1/2 hr/water quench)

TABLE III. - HYDROGEN ANALYSIS OF IRON-BASE ALLOYS

Alloy	Hydrogen content, ppm by weight		
	Before aging	After 3500 hr at 760° C hydrogen (30 to 60 kPa gage)	
		Before testing	After testing
N-155	5.4	3.9	3.4
19-9DL (HT-1)	3.4	6.9	6.0
19-9DL (HT-2)	1.6	4.7	4.6
316SS	.8	4.9	1.8
Nitronic 40	1.8	7.1	2.3
A286 (HT-1)	2.8	9.4	6.4
A286 (HT-2)	1.9	9.2	3.9
A286 (HT-3)	1.6	10.4	4.7
Incoloy 800H	.8	5.6	2.5
RA330	1.0	4.1	3.1

[a]H_2 aged and creep-rupture tested about 100 hr in air at 760° C.

TABLE IV. - GRAIN SIZE MEASUREMENTS OF IRON-BASE ALLOYS

Alloy	Average grain diameter, μm, prior to testing in the following conditions		
	Unaged	Aged in Ar	Aged in H_2
N-155	21	21	17
19-9DL (HT-1)	5	--	5
19-9DL (HT-2)	31	24	28
316SS	56	39	64
Nitronic 40	8	9	8
A286 (HT-1)	5	8	5
A286 (HT-2)	11	12	14
A286 (HT-3)	72	66	72
Incoloy 800H	70	85	83
RA330	32	34	36

TABLE V. - TENSILE PROPERTIES OF IRON-BASE ALLOYS

Alloy	Condition	25° C			425° C			760° C		
		YS, MPa	UTS, MPa	Elongation,[c] percent	YS, MPa	UTS, MPa	Elongation,[c] percent	YS, MPa	UTS, MPa	Elongation,[c] percent
N155	Unaged	367	751	42	239	528[a]	28[b]	165	365	19
	Ar aged	360	822[a]	19[b]	253	592[a]	15[b]	223	345	50
	H_2 aged	349	827	23	268	666[a]	19	212	345	52
19-9DL (HT-1)	Unaged	339	779	48	270	562	26	168	219	57
	Ar aged	331	694[a]	17[b]	219	443	16	137	200	41
	H_2 aged	326	661	13	262	519[a]	12[b]	159	221	75
19-9DL (HT-2)	Unaged	270	739	66	166	614	37[b]	127	345	18[b]
	Ar aged	232	746[a]	22[b]	157	439[a]	18	121	226	33
	H_2 aged	305	745	22	193	550	18	143	270	25
316SS	Unaged	217	552	63	92	400	36	68	188	80
	Ar aged	224	592	45	140	439	27	106	192	37
	H_2 aged	179	563	51	125	425	26	110	211	33
Nitronic 40	Unaged	434	827	58	263	576	41	180	271	38
	Ar aged	361	738[a]	12[b]	224	541	15	205	245	46
	H_2 aged	346	678[a]	8	221	507	12[b]	132	221	52
A286 (HT-1)	Unaged	734	1172	23	703	1041[a]	13	421	461	27
	Ar aged	371	745	26	276	634	18	198	273	39
	H_2 aged	403	752	21	313	638	18	208	292	46
A286 (HT-2)	Unaged	692	1153	25	651	1020	16	464	513	12[b]
	Ar aged	370	760	27	283	620	19	225	307	34
	H_2 aged	336	718	32	254	601	20	206	296	42
A286 (HT-3)	Unaged	308	539[a]	36[b]	147	344[a]	37	131	236	11
	Ar aged	332	697[a]	8[b]	245	608[a]	12	214	319	33[b]
	H_2 aged	321	720[a]	12	263	633[a]	22	213	334	24
Incoloy 800H	Unaged	161	559	42	97	467	36	127	228	33
	Ar aged	157	569	33[b]	100	437	30	80	212	44
	H_2 aged	159	566	36	98	445	28[b]	83	226	33[b]
RA330	Unaged	310	564	43	188	479	29	132	209	22
	Ar aged	216	556	43	160	446	35	114	186	63[d]
	H_2 aged	208	538	50	156	430	37	123	197	51

[a]Fracture strength.
[b]Broke at or outside gage mark.
[c]in 2.54 cm gage length.
[d]Estimated.

TABLE VI. - CREEP-RUPTURE DATA OF IRON-BASE ALLOYS

(a) Creep-rupture data for N-155.

Condition	Test temperature, °C	Stress, MPa	Minimum creep rate, sec^{-1}	Rupture life, hr	Elongation to rupture, percent
Unaged	705	276	4.63×10^{-7}	23.1	11
		207	4.15×10^{-8}	202.2	17
		172	2.04×10^{-8}	513.2	17
	760	207	2.37×10^{-6}	10.8	25
		172	3.84×10^{-7}	42.1	17
		138	9.44×10^{-8}	139.3	13
		124	3.90×10^{-8}	390.7	21
		103	1.36×10^{-8}	878.7	17
	815	207	2.57×10^{-5}	1.1	25
		172	5.94×10^{-6}	4.6	15
		138	1.48×10^{-6}	15.9	19
		103	2.16×10^{-7}	100.6	22
		83	3.56×10^{-8}	439.3	20
		69	2.76×10^{-9}	1450.6	20
	870	103	3.05×10^{-6}	9.5	31
		69	2.50×10^{-7}	117.4	29
Ar aged	760	138	4.20×10^{-7}	87.0	26
		103	3.55×10^{-8}	------	--
	815	103	3.55×10^{-7}	100.2	35
		83	7.39×10^{-8}	234.5	31
		69	1.39×10^{-8}	------	--
H_2 aged	760	138	7.48×10^{-7}	61.0	51
		103	9.54×10^{-8}	389.6	32
		90	2.12×10^{-8}	1110.0	36
	815	103	1.08×10^{-6}	40.7	53
		83	1.24×10^{-7}	218.9	37
		69	2.78×10^{-8}	625.8	25

TABLE VI. - CREEP-RUPTURE DATA OF IRON-BASE ALLOYS

(b) Creep-rupture data for 19-9DL (HT-1)

Condition	Test temperature, °C	Stress, MPa	Minimum creep rate, sec^{-1}	Rupture life, hr	Elongation to rupture, percent
Unaged	705	276	2.64×10^{-4}	------	---
		110	1.06×10^{-6}	------	112
		83	2.66×10^{-7}	------	68
		48	1.03×10^{-8}	1145.0	62
	760	110	1.16×10^{-5}	3.5	87
		90	3.44×10^{-6}	------	---
		62	1.60×10^{-6}	------	---
		48	5.81×10^{-7}	------	---
		28	---------	813.6	82
		28	4.19×10^{-8}	627.4	92
	815	48	4.54×10^{-6}	8.6	126
		28	9.22×10^{-7}	59.5	147
		14	3.82×10^{-8}	------	---
	870	28	5.46×10^{-6}	20.8	118
		14	1.08×10^{-6}	------	---
Ar aged	760	62	2.00×10^{-6}	41.1	80
		41	2.24×10^{-7}	------	---
		28	2.18×10^{-7}	535.8	140
	815	48	5.24×10^{-6}	15.1	91
		28	8.94×10^{-7}	142.8	128
H_2 aged	760	62	2.02×10^{-6}	36.5	89
		41	4.51×10^{-7}	204.7	76
		28	8.94×10^{-8}	810.2	92
	815	48	4.87×10^{-6}	------	---
		28	9.40×10^{-7}	------	---
		21	2.45×10^{-7}	389.2	143

TABLE VI. - CREEP-RUPTURE DATA OF IRON-BASE ALLOYS

(c) Creep-rupture data for 19-9DL (HT-2)

Condition	Test temperature, °C	Stress, MPa	Minimum creep rate, sec^{-1}	Rupture life, hr	Elongation to rupture, percent
Unaged	705	207	1.41×10^{-7}	77.5	21
		172	7.74×10^{-8}	------	---
		138	1.89×10^{-8}	1016.4	17
	760	138	2.28×10^{-7}	61.4	21
		117	1.47×10^{-7}	184.7	21
		97	3.01×10^{-8}	570.6	17
		83	1.35×10^{-8}	931.6	17
	815	97	3.48×10^{-7}	65.3	21
		83	1.65×10^{-7}	123.1	20
		62	1.83×10^{-8}	------	---
	870	62	5.07×10^{-7}	69.7	18
Ar aged	760	117	1.24×10^{-6}	35.3	30
		83	5.09×10^{-8}	417.0	15
	815	83	1.15×10^{-6}	34.1	23
		55	1.00×10^{-7}	------	---
H_2 aged	760	117	1.63×10^{-6}	33.6	32
		83	1.19×10^{-7}	343.8	22
	815	83	1.59×10^{-6}	33.7	37
		55	6.17×10^{-8}	------	---

TABLE VI. - CREEP-RUPTURE DATA OF IRON-BASE ALLOYS

(d) Creep-rupture data for 316SS

Condition	Test temperature, °C	Stress, MPa	Minimum creep rate, sec^{-1}	Rupture life, hr	Elongation to rupture, percent
Unaged	705	138	2.32×10^{-6}	30.0	63
		103	2.91×10^{-7}	188.4	47
		83	3.06×10^{-8}	1618.9	37
	760	138	--------	1.7	52
		103	4.50×10^{-6}	------	--
		69	5.55×10^{-7}	136.7	32
		55	1.14×10^{-7}	478.0	28
		48	5.44×10^{-8}	759.0	27
		41	2.10×10^{-8}	------	--
	815	69	--------	19.0	40
		69	3.91×10^{-6}	16.0	35
		48	7.11×10^{-7}	------	--
		41	4.18×10^{-7}	108.2	27
		35	1.07×10^{-7}	333.0	24
		28	6.40×10^{-8}	------	--
	870	35	2.43×10^{-6}	490.3	22
Ar aged	760	69	4.52×10^{-7}	96.3	21
		55	1.35×10^{-7}	262.3	20
		48	7.40×10^{-8}	428.4	23
	815	35	2.00×10^{-7}	199.2	41
		21	1.33×10^{-8}	1658.1	23
H_2 aged	760	69	6.99×10^{-7}	------	--
		55	1.88×10^{-7}	258.1	42
		41	2.70×10^{-8}	2067.9	25
		41	5.96×10^{-8}	729.0	39
	815	35	1.66×10^{-7}	267.0	42
		28	7.03×10^{-8}	455.2	39

TABLE VI. - CREEP-RUPTURE DATA OF IRON-BASE ALLOYS

(e) Creep-rupture data for Nitronic 40

Condition	Test temperature, °C	Stress, MPa	Minimum creep rate, sec^{-1}	Rupture life, hr	Elongation to rupture, percent
Unaged	705	172	8.08×10^{-7}	33.1	25
		138	--------	77.9	45
		110	9.44×10^{-8}	180.7	53
		83	5.34×10^{-8}	409.1	51
		55	1.08×10^{-8}	1529.3	54
	760	110	7.11×10^{-7}	------	--
		110	9.20×10^{-7}	------	61
		83	3.26×10^{-7}	------	57
		55	1.15×10^{-7}	246.1	60
		35	5.11×10^{-8}	693.2	97
	815	83	2.76×10^{-6}	------	100
		69	1.58×10^{-6}	21.6	84
		55	4.33×10^{-7}	------	84
		35	2.00×10^{-7}	152.1	93
		21	6.29×10^{-8}	465.0	117
	870	21	5.30×10^{-7}	103.0	105
		10	2.29×10^{-7}	583.1	172
Ar aged	760	55	2.78×10^{-7}	------	---
		35	5.31×10^{-8}	730.9	89
	815	35	4.46×10^{-7}	114.9	112
		21	9.07×10^{-8}	394.4	132
H_2 aged	760	35	3.46×10^{-7}	200.8	121
		28	2.00×10^{-7}	429.8	108
		21	1.00×10^{-7}	857.4	108
	815	41	3.18×10^{-6}	27.4	117
		21	5.93×10^{-7}	192.3	140

TABLE VI. - CREEP-RUPTURE DATA OF IRON-BASE ALLOYS

(f) Creep-rupture data for A286 (HT-1)

Condition	Test temperature, °C	Stress, MPa	Minimum creep rate, sec^{-1}	Rupture life, hr	Elongation to rupture, percent
Unaged	705	276	3.83×10^{-7}	34.9	30
		207	1.10×10^{-7}	------	---
		138	4.59×10^{-8}	389.6	28
		55	3.52×10^{-9}	------	---
	760	207	1.11×10^{-6}	------	---
		138	4.32×10^{-7}	40.1	50
		103	2.65×10^{-7}	59.2	38
		69	6.94×10^{-8}	222.4	39
		55	3.02×10^{-8}	432.1	20
		41	3.42×10^{-8}	387.4	(58)
		31	2.68×10^{-8}	------	---
		21	1.23×10^{-8}	------	---
	815	138	2.24×10^{-5}	1.76	62
		103	6.98×10^{-6}	5.7	62
		69	4.75×10^{-6}	9.7	108
		41	2.24×10^{-7}	126.6	44
		28	1.28×10^{-7}	------	---
		21	8.14×10^{-8}	------	---
		14	4.07×10^{-8}	------	---
	870	28	1.70×10^{-6}	29.4	125
		14	4.89×10^{-7}	347.4	58
Ar aged	760	103	3.48×10^{-7}	103.8	41
		69	3.78×10^{-8}	------	---
		55	3.69×10^{-8}	------	---
		41	4.34×10^{-8}	------	---
	815	41	2.90×10^{-7}	------	---
		28	8.19×10^{-8}	602.4	45
H_2 aged	760	103	6.98×10^{-7}	54.5	45
		69	2.29×10^{-7}	183.5	54
		41	3.34×10^{-8}	1421.0	50
		21	2.55×10^{-8}	------	---
	815	41	3.55×10^{-7}	------	---
		28	1.28×10^{-7}	379.0	45

TABLE VI. - CREEP-RUPTURE DATA OF IRON-BASE ALLOYS

(g) Creep-rupture data for A286 (HT-2)

Condition	Test temperature, °C	Stress, MPa	Minimum creep rate, sec^{-1}	Rupture life, hr	Elongation to rupture, percent
Unaged	705	207	5.69×10^{-8}	182.6	28
		172	3.04×10^{-8}	-----	--
		138	1.01×10^{-8}	-----	--
	760	172	3.48×10^{-7}	30.0	43
		138	1.66×10^{-7}	58.9	29
		103	5.42×10^{-8}	169.7	28
		69	1.55×10^{-8}	707.4	14
		55	1.48×10^{-8}	-----	--
		35	1.17×10^{-8}	-----	--
		21	2.21×10^{-9}	-----	--
	815	83	2.85×10^{-7}	35.4	41
		55	6.51×10^{-8}	144.3	29
		35	5.08×10^{-8}	-----	--
		21	1.92×10^{-8}	-----	--
	870	55	8.10×10^{-6}	-----	--
		35	1.74×10^{-6}	41.4	66
		21	1.87×10^{-9}	-----	--
Ar aged	760	138	6.05×10^{-7}	52.3	40
		138	7.62×10^{-7}	-----	--
		103	2.82×10^{-8}	430.0	35
		69	2.18×10^{-8}	-----	--
	815	55	9.73×10^{-8}	138.4	40
		35	4.02×10^{-8}	-----	--
H_2 aged	760	138	2.94×10^{-6}	-----	--
		103	4.30×10^{-7}	90.6	47
		69	5.07×10^{-8}	-----	--
	815	55	2.36×10^{-7}	-----	--
		35	7.24×10^{-8}	977.2	43
		21	2.11×10^{-8}	-----	--

TABLE VI. - CREEP-RUPTURE DATA OF IRON-BASE ALLOYS

(h) Creep-rupture data for A286 (HT-3)

Condition	Test temperature, °C	Stress, MPa	Minimum creep rate, sec^{-1}	Rupture life, hr	Elongation to rupture, percent
Unaged	705	345	1.18×10^{-7}	------	--
		310	1.22×10^{-8}	136.9	1
		276	3.27×10^{-9}	292.2	2
	760	303	3.82×10^{-7}	9.3	6
		276	1.65×10^{-7}	16.3	8
		207	1.28×10^{-8}	85.9	12
		138	1.20×10^{-9}	342.0	10
		103	9.60×10^{-10}	665.3	7
	815	152	1.59×10^{-7}	12.6	15
		103	1.04×10^{-7}	48.5	22
		83	2.74×10^{-8}	109.9	22
		62	5.69×10^{-9}	427.7	12
		55	5.63×10^{-9}	------	--
		41	2.15×10^{-9}	------	--
	870	41	2.58×10^{-7}	56.6	37
		24	3.45×10^{-8}	3625.1	23
	925	24	7.73×10^{-7}	------	--
Ar aged	760	207	1.30×10^{-5}	2.4	28
		138	9.40×10^{-7}	------	--
		138	8.61×10^{-7}	42.2	26
		103	1.27×10^{-7}	------	--
	815	83	3.79×10^{-7}	82.8	17
		62	6.82×10^{-8}	462.8	19
H_2 aged	760	207	2.64×10^{-5}	------	--
		138	4.14×10^{-7}	45.0	25
		103	8.96×10^{-8}	------	--
		83	1.02×10^{-8}	------	--
	815	103	5.32×10^{-7}	------	--
		83	3.95×10^{-7}	71.6	19
		62	5.46×10^{-8}	433.4	10

TABLE VI. - CREEP-RUPTURE DATA OF IRON-BASE ALLOYS

(i) Creep-rupture data for Incoloy 800H

Condition	Test temperature, °C	Stress, MPa	Minimum creep rate, sec^{-1}	Rupture life, hr	Elongation to rupture, percent
Unaged	705	152	5.16×10^{-7}	------	--
		124	1.69×10^{-7}	------	--
		103	5.32×10^{-8}	------	--
	760	124	1.96×10^{-6}	------	--
		103	5.99×10^{-7}	------	--
		103	7.47×10^{-7}	59.9	28
		83	1.44×10^{-7}	216.3	23
		69	4.44×10^{-8}	------	--
		62	2.53×10^{-8}	1307.5	28
	815	124	7.26×10^{-5}	.95	70
		103	3.23×10^{-5}	2.5	79
		69	2.76×10^{-6}	33.5	54
		55	4.38×10^{-7}	93.5	32
		41	3.62×10^{-8}	960.4	22
	870	41	3.84×10^{-7}	102.3	30
		31	1.03×10^{-7}	425.7	27
Ar aged	760	83	1.38×10^{-7}	------	--
		83	1.29×10^{-6}	68.4	57
		69	3.41×10^{-7}	151.3	40
		62	9.84×10^{-8}	538.5	29
	815	55	4.20×10^{-7}	------	--
		41	8.61×10^{-8}	457.5	24
H_2 aged	760	83	1.58×10^{-6}	------	--
		69	4.47×10^{-7}	212.9	60
		62	1.68×10^{-7}	525.8	58
	815	55	6.03×10^{-7}	------	--
		41	8.90×10^{-8}	400.8	29

TABLE VI. - CREEP-RUPTURE DATA OF IRON-BASE ALLOYS

(j) Creep-rupture data for RA-330

Condition	Test temperature, °C	Stress, MPa	Minimum creep rate, sec^{-1}	Rupture life, hr	Elongation to rupture, percent
Unaged	705	138	3.77×10^{-6}	-----	--
		103	6.07×10^{-7}	91.0	50
		83	1.26×10^{-7}	-----	45
	760	103	7.05×10^{-6}	9.9	40
		69	4.74×10^{-7}	92.1	30
		55	5.13×10^{-8}	428.0	41
		41	4.59×10^{-9}	-----	--
	815	103	1.25×10^{-4}	-----	58
		55	8.08×10^{-7}	57.4	48
		41	6.03×10^{-8}	-----	--
		35	5.78×10^{-9}	194.5	27
		35	3.20×10^{-8}	555.9	43
	870	35	4.30×10^{-8}	96.7	31
		28	3.41×10^{-8}	210.0	24
Ar aged	760	69	5.80×10^{-7}	111.9	51
		55	5.85×10^{-8}	431.1	42
	815	41	2.02×10^{-8}	-----	--
		35	4.86×10^{-9}	-----	--
H_2 aged	760	69	9.38×10^{-7}	72.4	50
		55	2.57×10^{-7}	198.6	35
		41	5.36×10^{-8}	681.9	51
	815	41	2.69×10^{-7}	93.8	40
		35	4.86×10^{-8}	-----	--

TABLE VII. - MULTIPLE LINEAR REGRESSION ANALYSIS OF CREEP AND RUPTURE LIFE OF UNAGED IRON-BASE ALLOYS[a]

Alloy	Minimum creep rate data					Rupture life data				
	Stress range, MPa	Correlation coefficient, R^2	Activation energy Q_1, kJ/mol	Stress-term exponent, n_1	ln k_1	Stress range, MPa	Correlation coefficient, R^2	Activation energy Q_2, kJ/mol	Stress-term exponent, n_2	ln k_2
N-155	69-276	0.973	-502.0	7.45	5.39	69-276	0.995	400.0	-6.40	-10.10
19-9DL (HT-1)	14-110	.957	-454.8	3.97	22.96	28-110	.985	355.7	-3.85	-22.05
19-9DL (HT-2)	62-207	.952	-417.0	5.90	4.40	62-207	.971	357.3	-5.40	-10.77
316SS	83-138	.994	-450.7	8.41	1.06	69-138	.985	439.6	-6.99	-16.16
	28-69	.972	-470.5	5.77	15.53	28-55	.940	396.6	-3.63	-25.39
Nitronic 40	69-172	.969	-321.1	3.53	6.99	69-172	.977	290.1	-3.44	-14.38
	10-55	.953	-289.0	1.50	11.34	10-55	.997	275.8	-2.36	-17.11
A286 (HT-1)	55-276	.952	-484.2	2.86	8.50	14-276	.956	400.4	-3.05	-7.40
	14-41	.974	-378.3	1.59	9.85					
A286 (HT-2)	83-207	.997	-406.1	3.81	12.86	34-276	.970	413.8	-3.44	-27.19
	21-69[b]	.922	-298.0	1.46	10.77					
A286 (HT-3)	276-345	.973	-557.3	14.87	-34.58	24-310	.924	472.2	-4.13	-29.10
	24-207	.963	-766.1	3.52	51.76					
Incoloy 800H	31-152	.968	-511.8	6.84	14.01	31-103	.991	480.4	-6.33	-22.69
RA-330	28-138	.967	-401.3	8.02	-2.16	28-103	.905	304.4	-4.79	-10.63

[a]From equations (1) and (2) in text.
[b]Excluding 870° C data.

(a) N-155.

(b) 316SS.

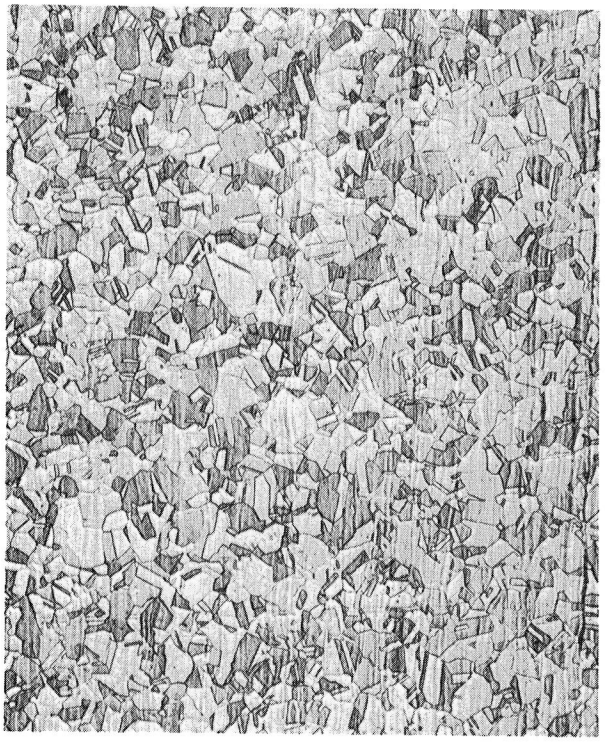

(c) Nitronic 40.

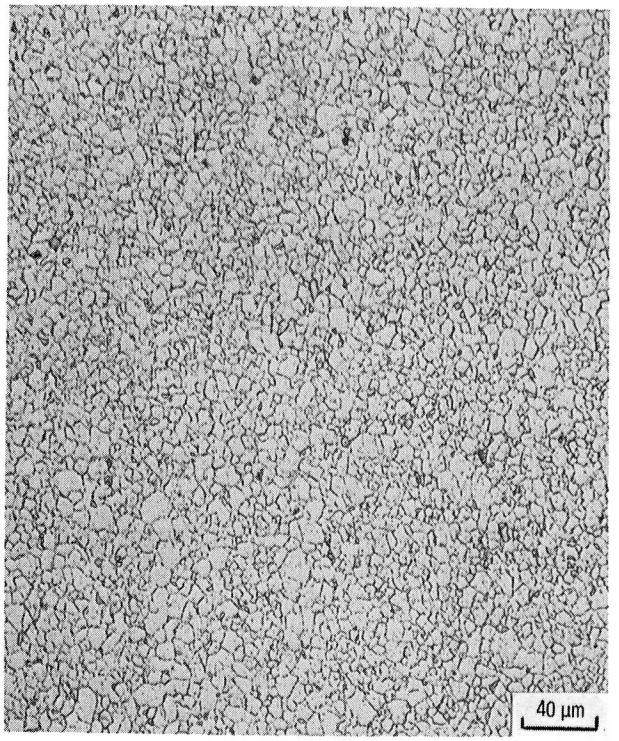

(d) A286 (HT-1).

Figure 1. - Microstructures of unaged alloys.

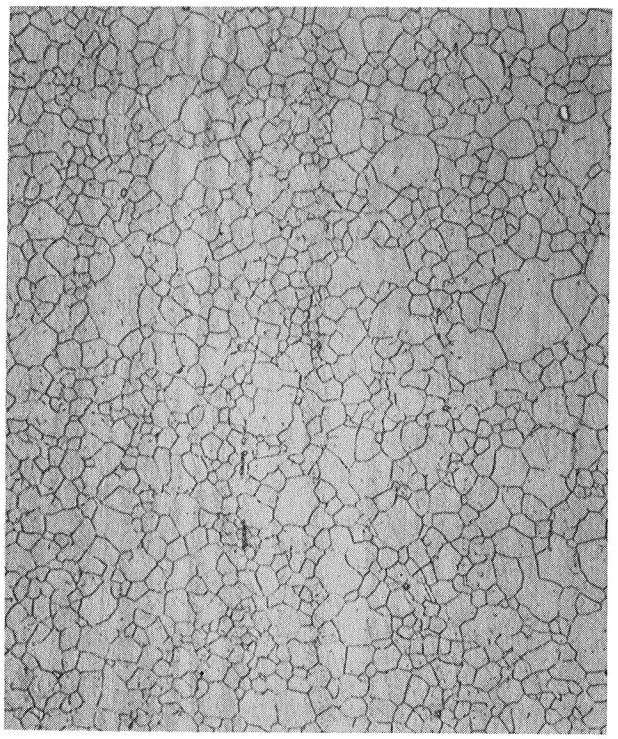

(e) A286 (HT-2).

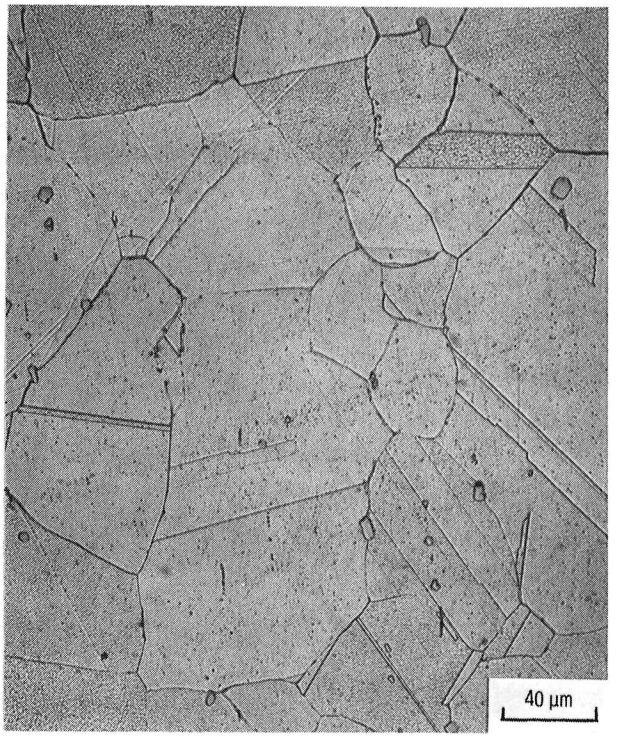

(f) A286 (HT-3).

(g) Incoloy 800.

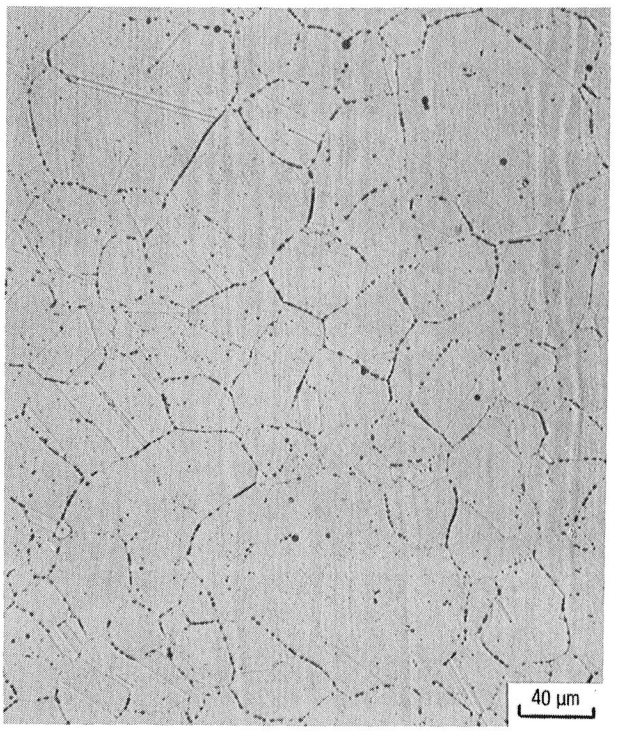

(h) RA330.

Figure 1. - Concluded.

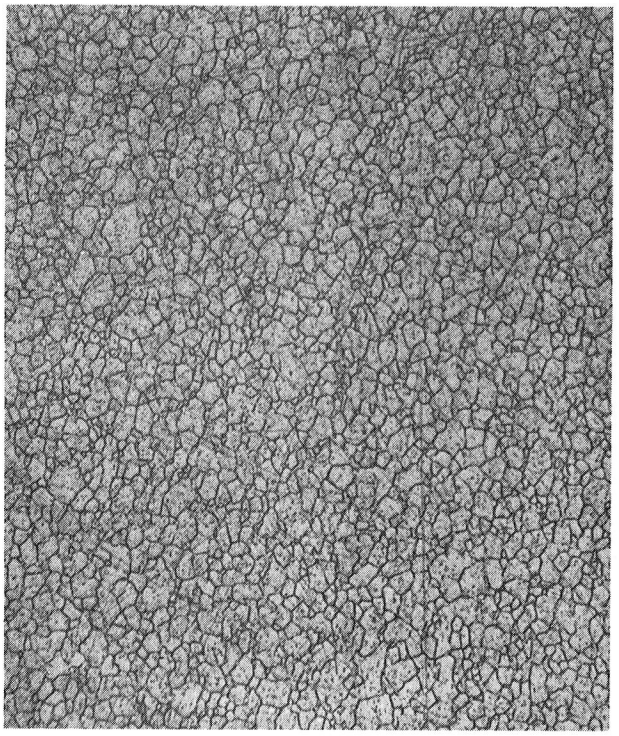

(a) HT-1 unaged.

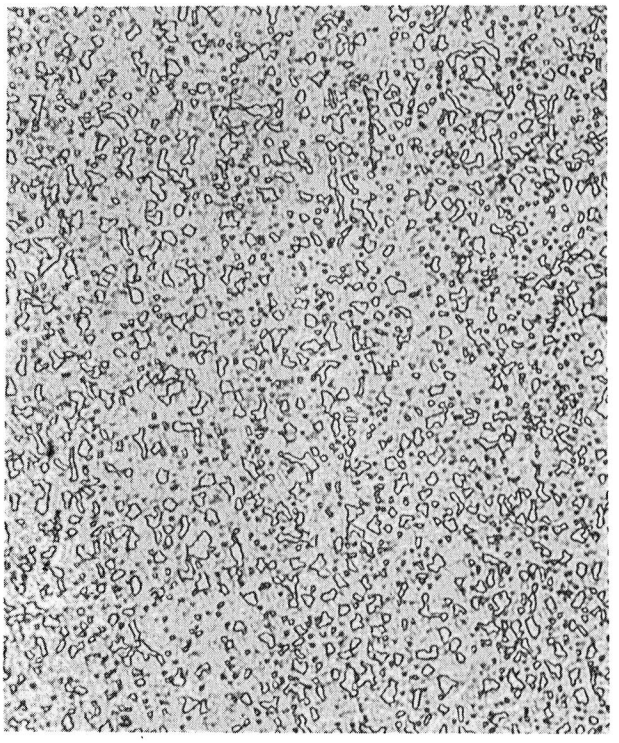

(b) HT-1 Ar aged.

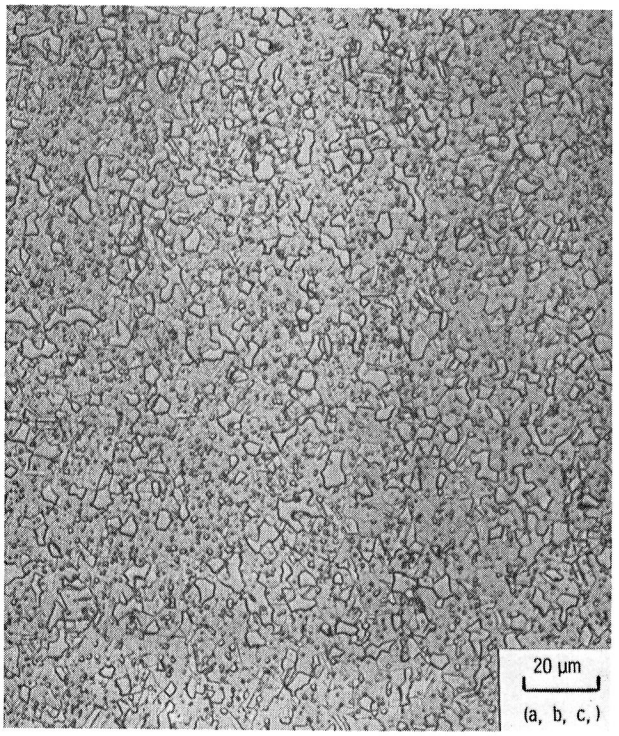

(c) HT-1 H_2 aged.

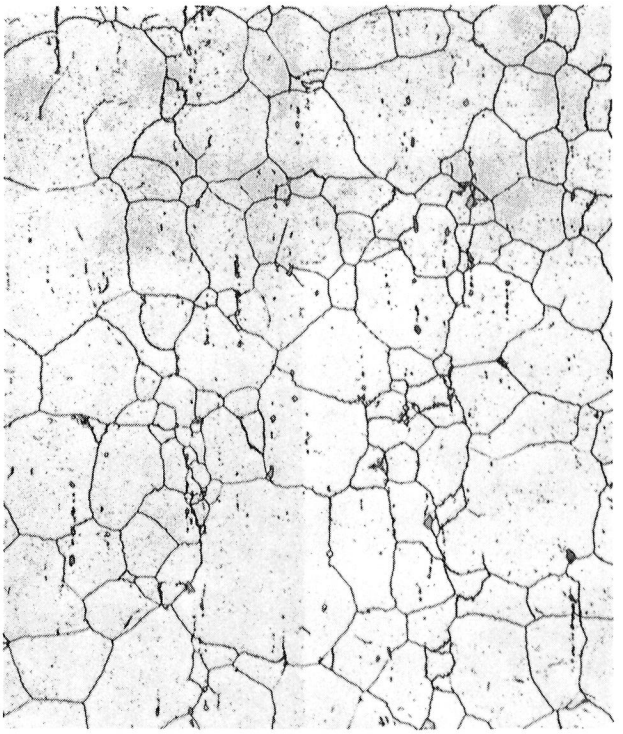

(d) HT-2 unaged.

Figure 2. - Microstructure of 19-9DL alloy for two heat treatments, before and after long term aging in argon and in hydrogen.

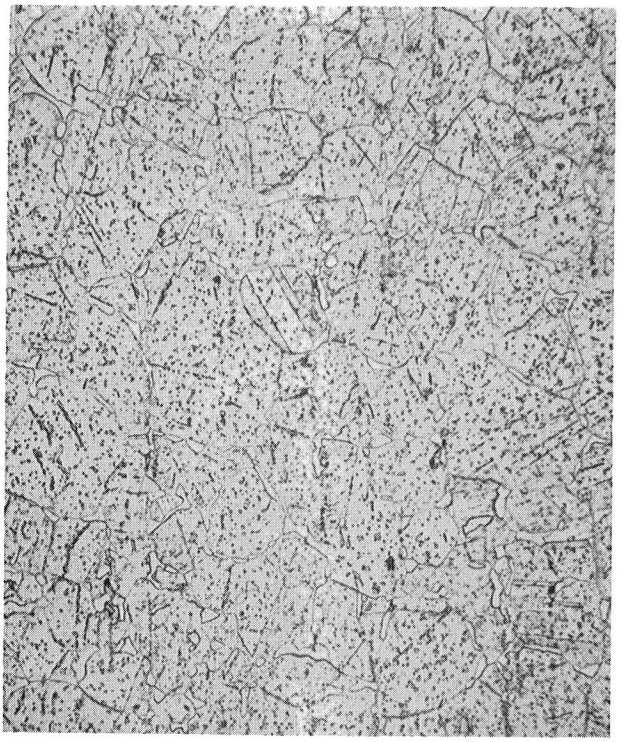

(e) HT-2 Ar aged.

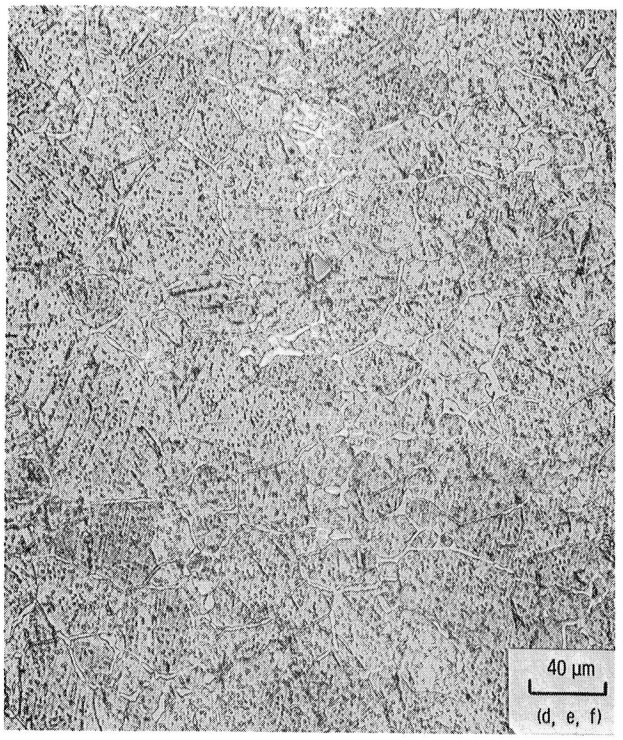

(f) HT-2 H_2 aged.

Figure 2. - Concluded.

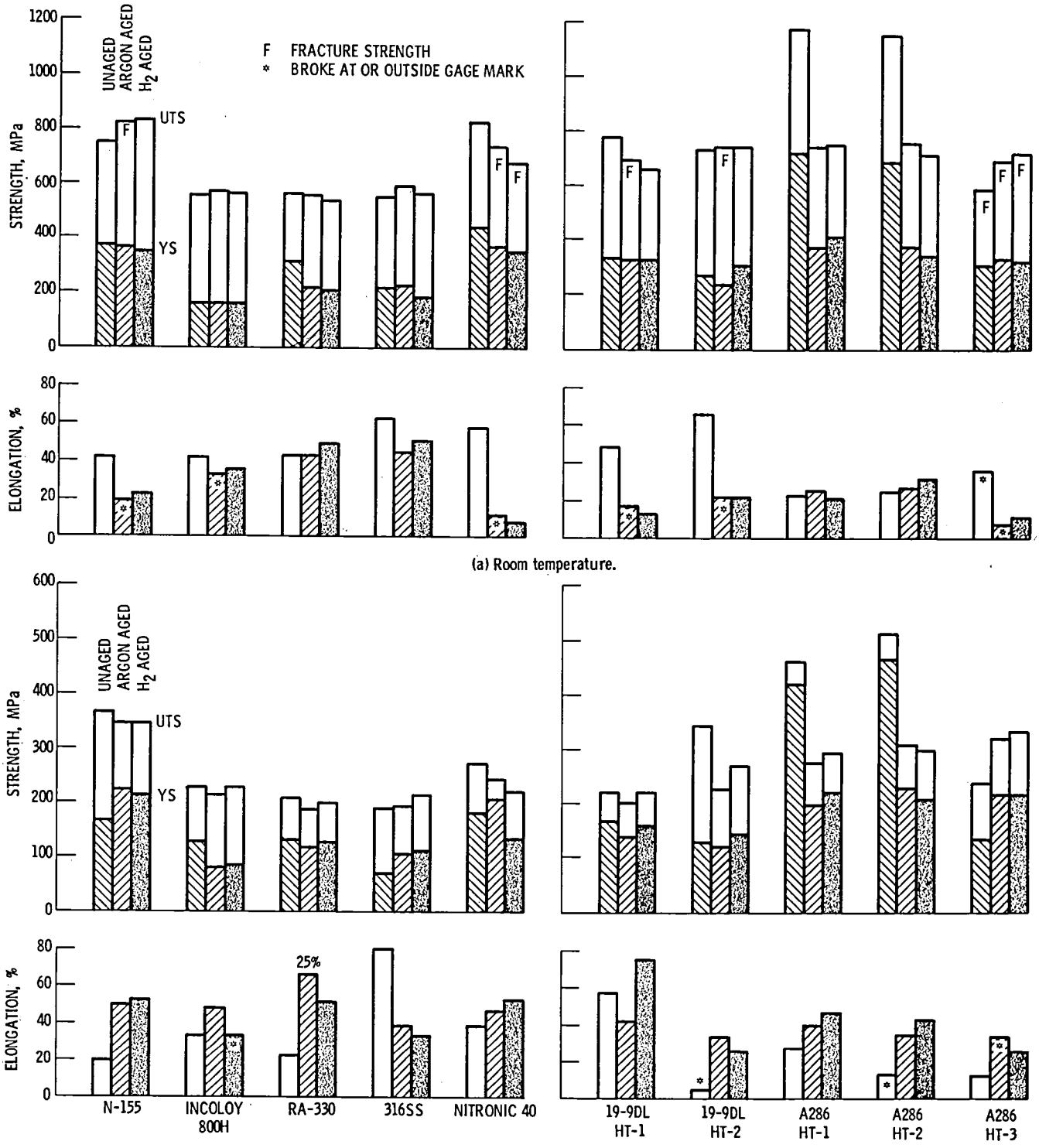

(a) Room temperature.

(b) Temperature at 760° C.

Figure 3. - Tensile properties of the iron-base alloys in the unaged, Ar aged, and H_2 aged conditions.

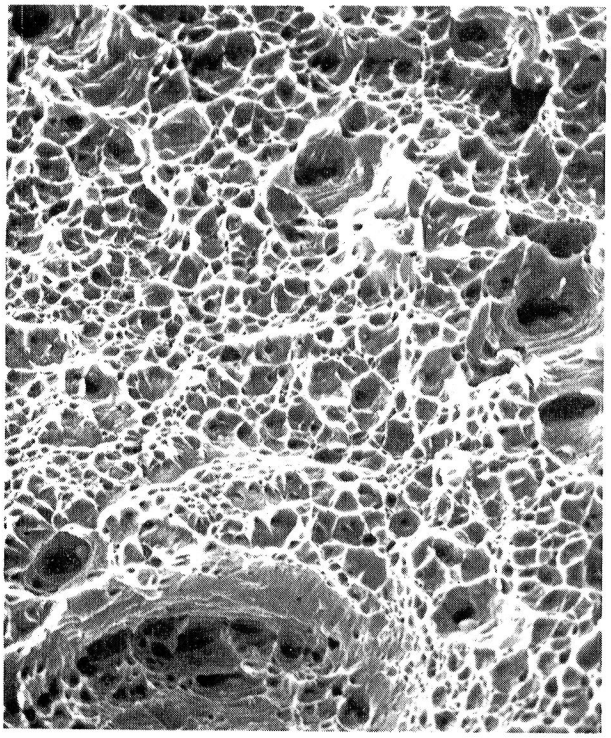

(a) Nitronic 40, unaged.

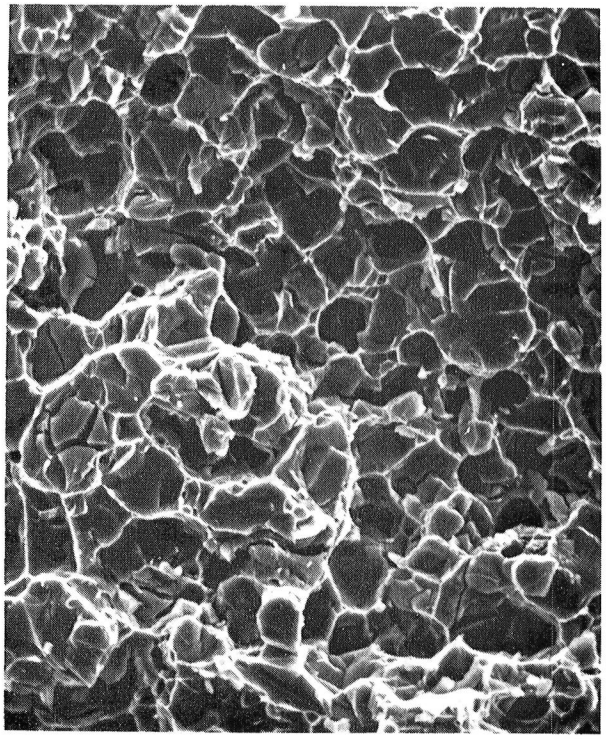

(b) Nitronic 40, H_2 aged.

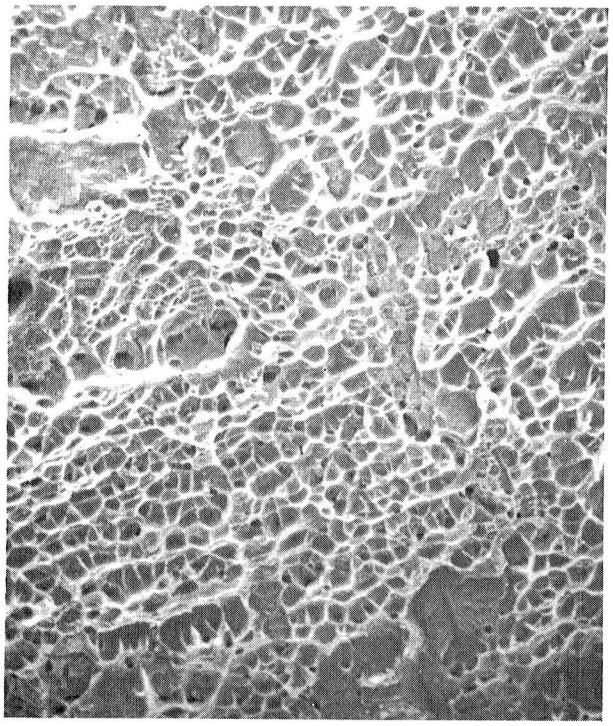

(c) A286 (HT-3), unaged.

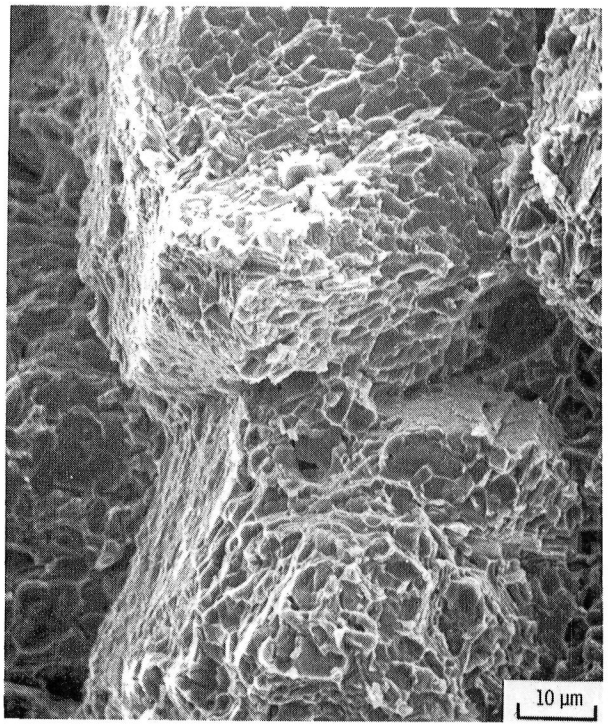

(d) A286 (HT-3), H_2 aged.

Figure 4. - Fracture surfaces of room temperature tensile specimens of Nitronic 40 and A286 alloys.

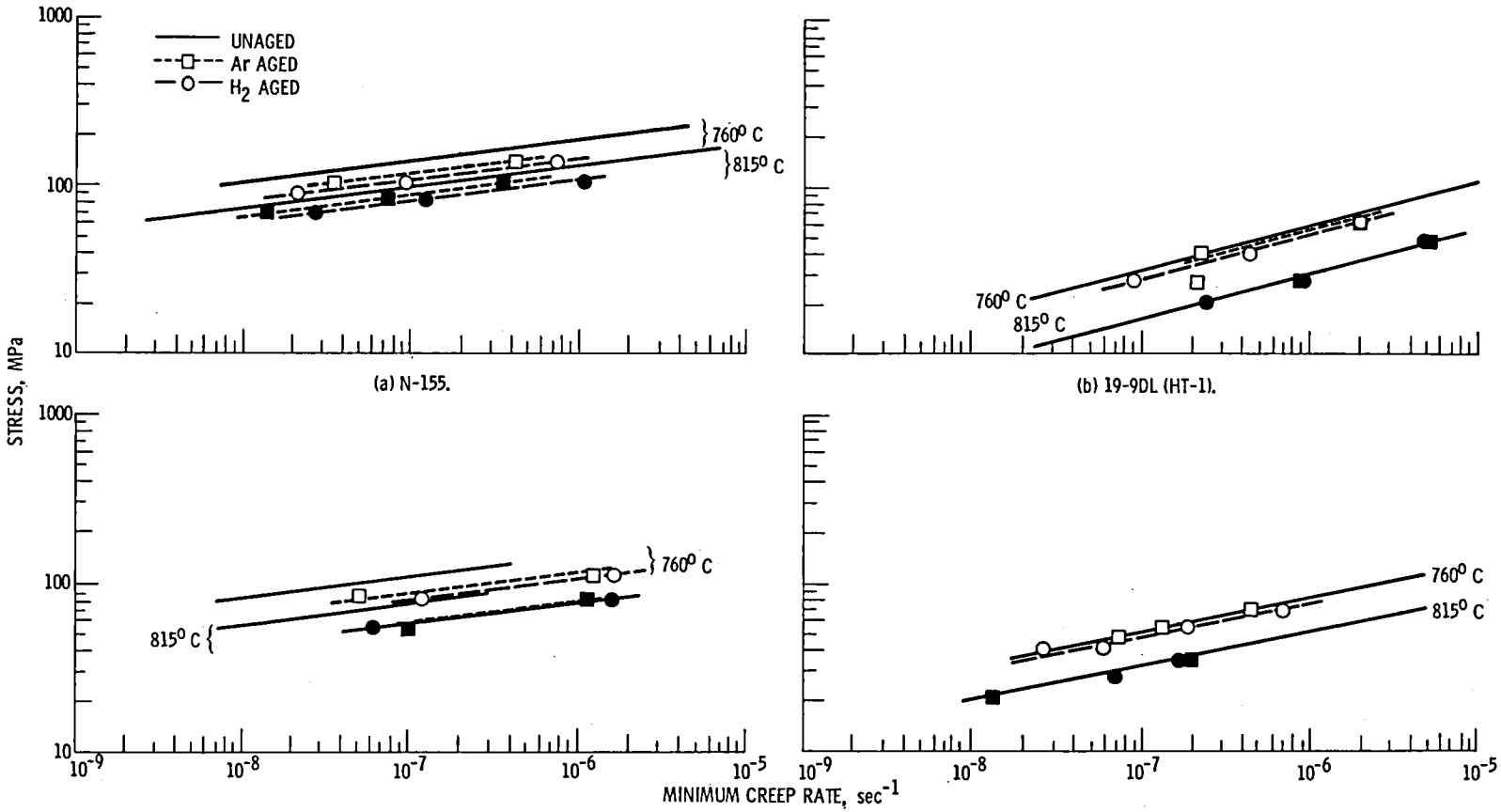

Figure 5. - Minimum creep rates for various iron-base alloys in the unaged and aged conditions at 760 and 815° C.

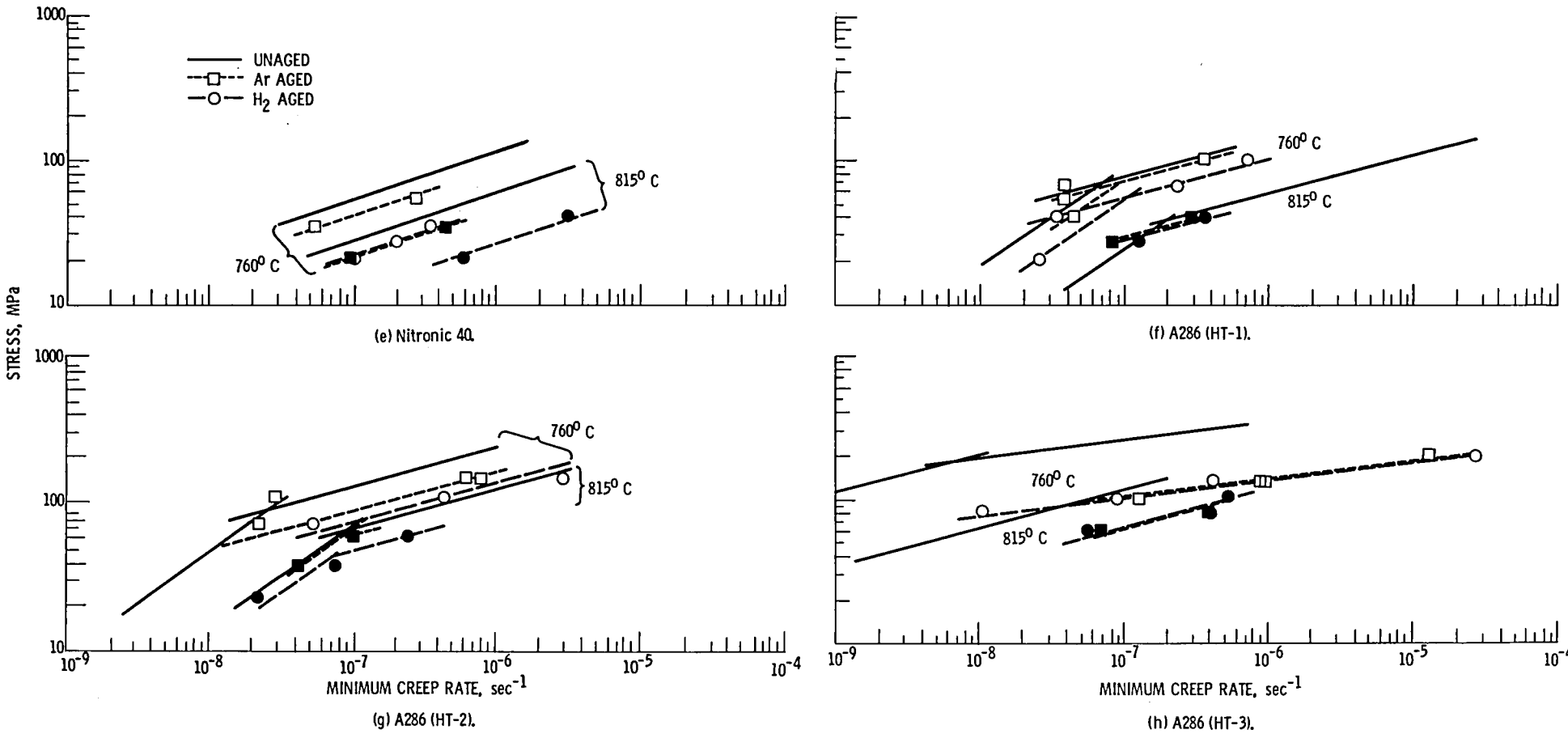

(e) Nitronic 40.

(f) A286 (HT-1).

(g) A286 (HT-2).

(h) A286 (HT-3).

Figure 5. - Continued.

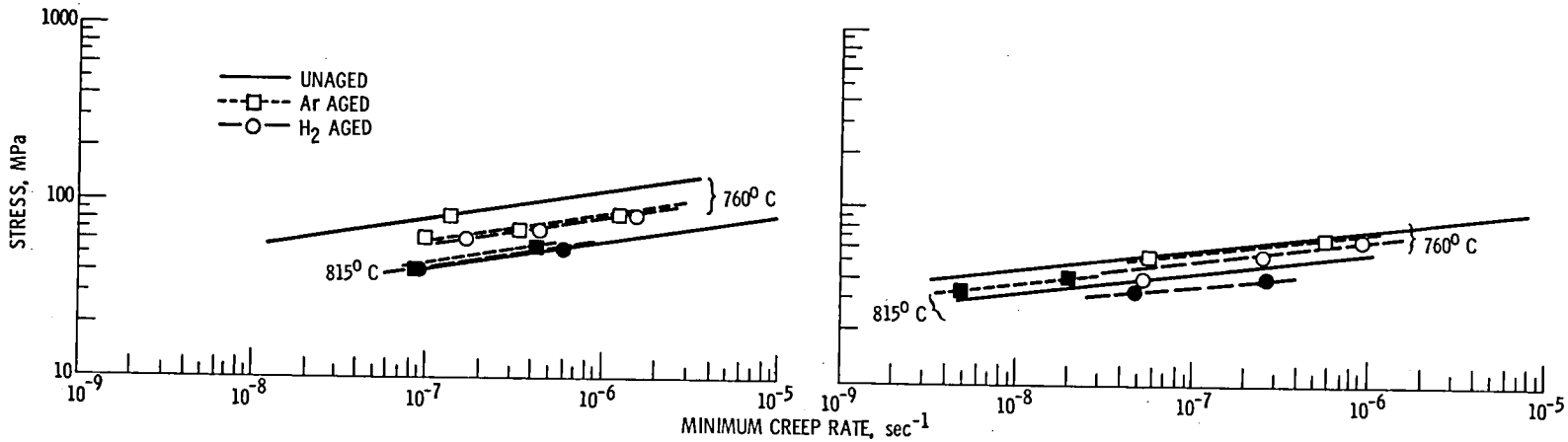

(i) Incoloy 800 H.

(j) RA330.

Figure 5. - Concluded.

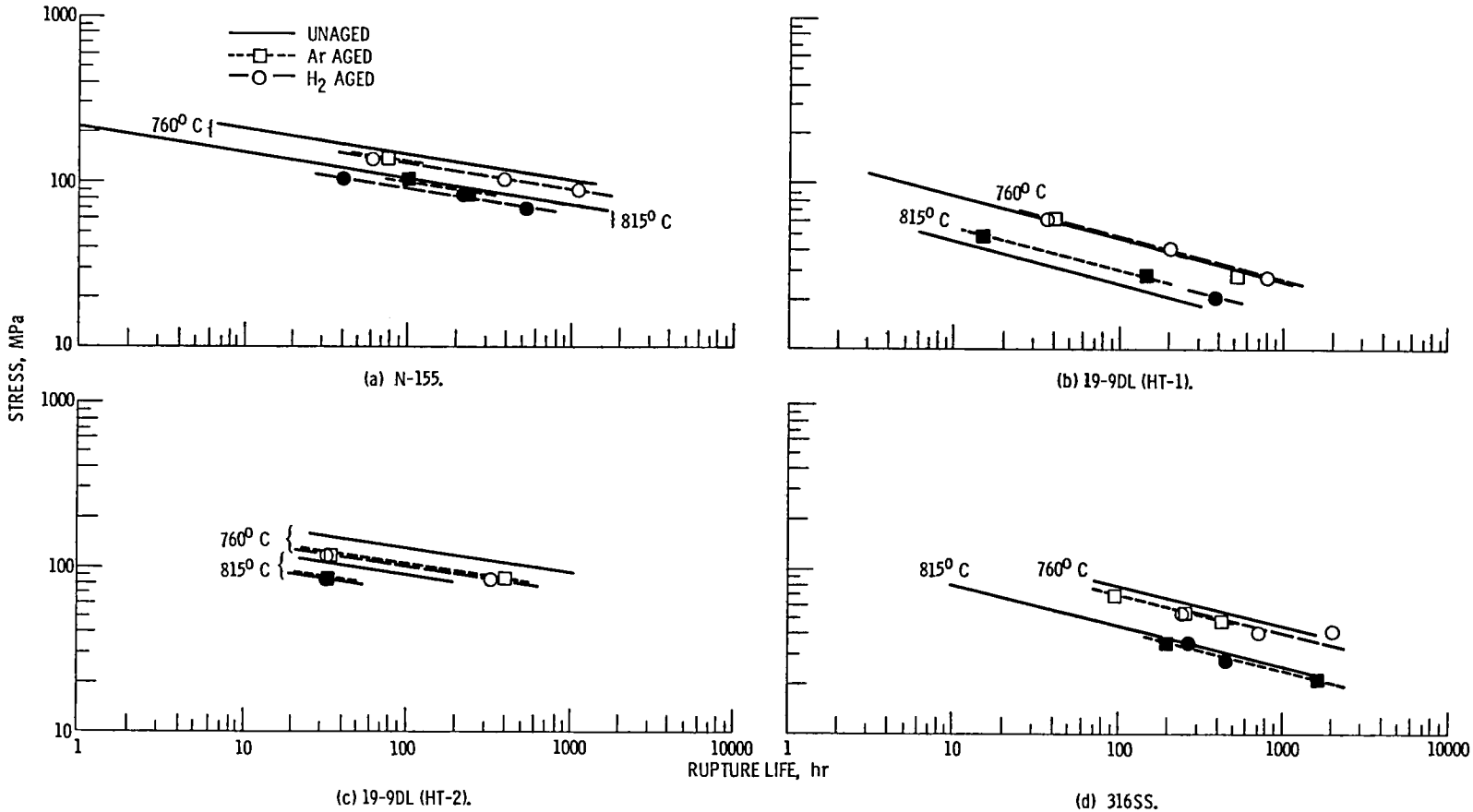

Figure 6. - Stress-rupture behavior of various iron-base alloys in the unaged and aged conditions at 760 and 815° C.

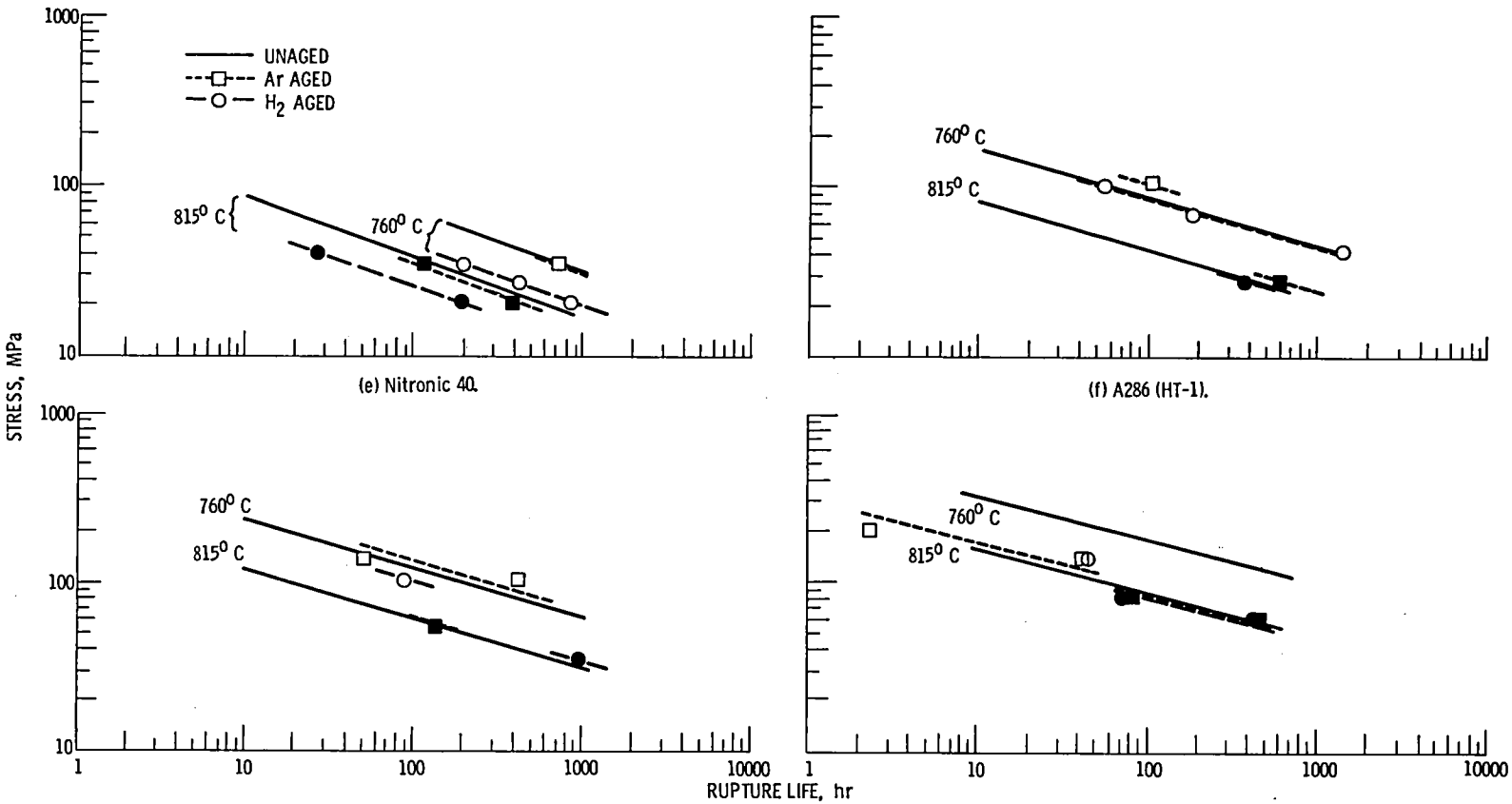

(e) Nitronic 40.

(f) A286 (HT-1).

(g) A286 (HT-2).

(h) A286 (HT-3).

Figure 6. - Continued.

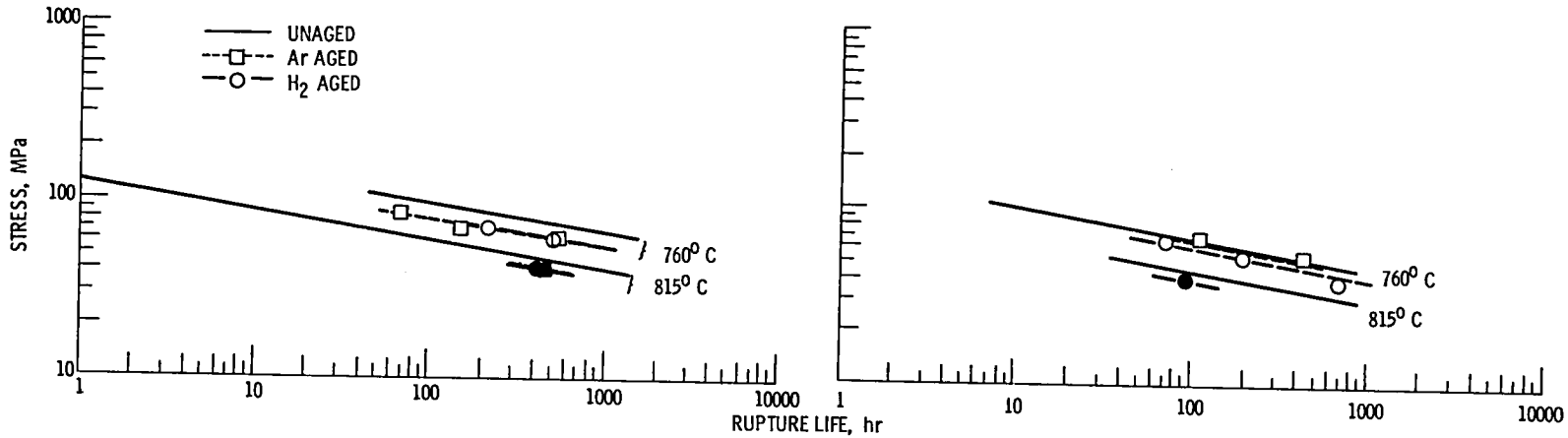

(i) Incoloy 800H.

(j) RA330.

Figure 6. - Concluded.

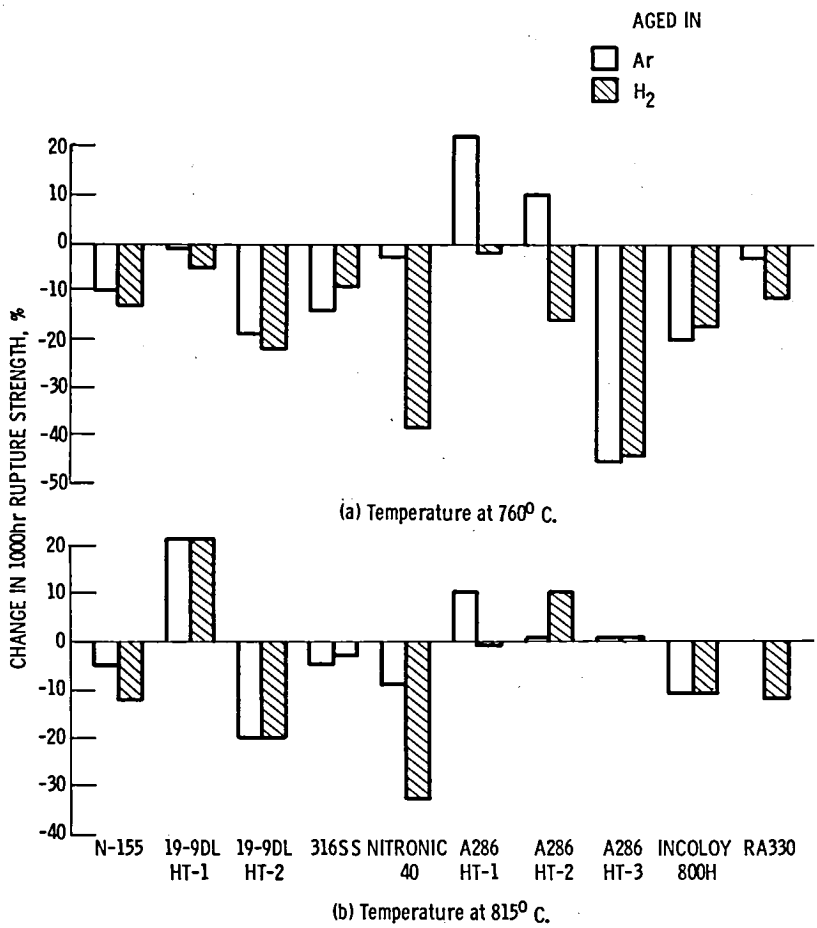

Figure 7. - Change in rupture strength of alloys at 760 and 815° C after long term aging in argon or hydrogen.

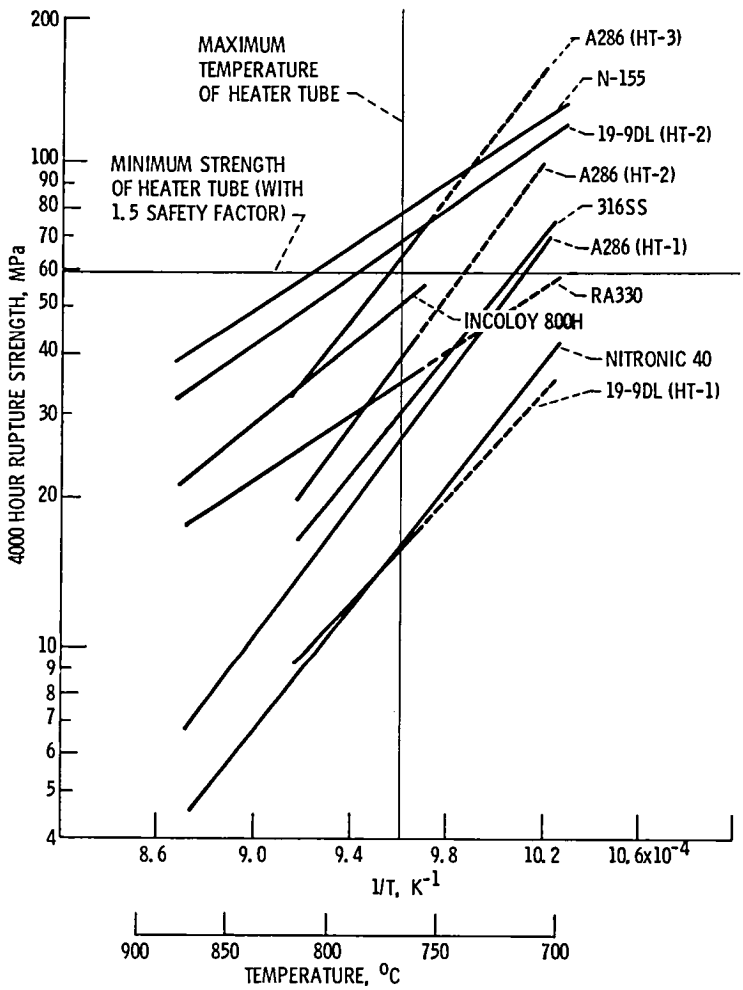

Figure 8. - The temperature dependency of rupture strength for unaged iron-base alloys compared to the Mod I Stirling automotive engine requirements for heater tubes.

1. Report No.	2. Government Accession No.	3. Recipient's Catalog No.
NASA TM-81534		

4. Title and Subtitle	5. Report Date
CREEP-RUPTURE BEHAVIOR OF SEVEN IRON-BASE ALLOYS AFTER LONG TERM AGING AT 760° C IN LOW PRESSURE HYDROGEN	August 1980
	6. Performing Organization Code
7. Author(s)	8. Performing Organization Report No.
Walter R. Witzke and Joseph R. Stephens	E-486
	10. Work Unit No.
9. Performing Organization Name and Address	
National Aeronautics and Space Administration Lewis Research Center Cleveland, Ohio 44135	11. Contract or Grant No.
	13. Type of Report and Period Covered
12. Sponsoring Agency Name and Address	Technical Memorandum
U.S. Department of Energy Office of Transportation Programs Washington, D.C. 20545	14. Sponsoring Agency Code Report No. DOE/NASA/1040-15

15. Supplementary Notes

Final report. Prepared under Interagency Agreement EC-77-A-31-1040.

16. Abstract

Seven candidate iron-base alloys for heater tube application in the Stirling automotive engine were aged for 3500 hours at 760° C in argon and hydrogen. Aging degraded the tensile and creep-rupture properties. The presence of hydrogen during aging caused additional degradation of the rupture strength in fine grain alloys. Based on current design criteria for the Mod 1 Stirling engine, N-155 and 19-9DL are considered the only alloys in this study with strengths adequate for heater tube service at 760° C.

17. Key Words (Suggested by Author(s))	18. Distribution Statement
Creep; Rupture life; Aging effects; Stirling engine; Heater head; Activation energy; Tensile properties; Microstructure; Iron-base alloys; Heat resisting alloys	Unclassified - unlimited STAR Category 26 DOE Category UC-25

19. Security Classif. (of this report)	20. Security Classif. (of this page)	21. No. of Pages	22. Price*
Unclassified	Unclassified		

* For sale by the National Technical Information Service, Springfield, Virginia 22161